Acoustically Relevant Bubble Assemblages and Their Dependence on Meteorological Parameters

EDWARD C. MONAHAN AND MINGZHI LU

(*Invited Paper*)

Abstract—**A detailed physical model of the life history of a typical bubble plume, from its formation by a breaking wave to its dissipation into the background bubble population, is set down, and the relationship between the early, acoustically relevant stages in bubble-plume development and the associated, remotely detectable whitecap is described. The manner in which the fraction of the sea surface covered by Stage A spilling crests and by Stage B mature whitecaps depends upon wind speed and upon wind stress or "friction velocity" is investigated. Formal expressions are given whereby near-surface bubble concentrations can be estimated from observations of fractional whitecap coverage or from measurements of the 10-m elevation wind speed.**

I. Introduction

IT HAS long been recognized that air bubbles often occur in sufficient abundance in the near-surface layer of the ocean to appreciably alter the speed of sound [1] in this layer and thus give rise to acoustic refraction in the vicinity of the sea surface. Recently, attention has been paid to the role played by individual bubbles [2], [3], and by subsurface bubble assemblages [4], [5] as radiators of sound.

In the following section, the life history of a bubble plume, from its formation at the instant of wave breaking to its ultimate disappearance into the diffuse background bubble population, will be described, with particular attention being paid to the relationship between the early stages in the evolution of subsurface bubble plumes and the oceanic whitecaps that are the remotely monitorable [6] surface manifestations of these young plumes. In another section, the dependence of oceanic whitecap coverage on the 10-m elevation wind speed and alternatively on the magnitude of the wind stress upon the sea surface or "friction velocity" will be presented, and a model which can be used to estimate the near-surface bubble concentration from a knowledge of the whitecap coverage will be reviewed and expanded upon in the concluding section.

Manuscript revised May 1, 1990. The investigation of whitecaps and other bubble assemblages relevant to near-surface acoustic reverberation now being carried out at the University of Connecticut has been made possible by Office of Naval Research (ONR) Grant N00014-90-J-1538. Preliminary work on this topic was supported by ONR Award N00014-89-J-3176. The complementary research on whitecaps, dissolved gases, bubble survival, and aerosol production has been supported throughout by the ONR, most recently under Contract No. N00014-87-K-0185. This paper represents Marine Sciences Institute Contribution No. 222.

The authors are with the Marine Sciences Institute, University of Connecticut, Avery Point, Groton, CT 06340.

IEEE Log Number 9037871.

II. Biography of a Bubble Plume

The various stages in the evolution of a plume of air bubbles are illustrated in Fig. 1, which is intended to depict in one sketch both those visual features of the sea surface that are apparent to airborne and shipboard observers, and those subsurface features amenable to detection by either visual or acoustic means. It should be noted that in order to provide the viewer simultaneously with a "downward look" at the surface features and an "upward look" at the subsurface features, the bubble-impregnated block of mixed layer water in this figure has been rotated 90° with respect to the plane of the sea surface in the direction indicated by the curved arrow. The anchors-*cum*-plumb bobs are included in Fig. 1 to give a vertical reference in each of the two "hinged" portions of this figure. This particular figure represents an idiosyncratic assimilation of the perceptions shared among the participants in the 1987 NATO Advanced Research Workshop on Natural Mechanisms of Surface-Generated Noise in the Ocean held at Lerici, Italy, and incorporates one or more features borrowed from the earlier graphic representations of [7], [8] and [9], [10]. A concerted effort has been made to render the sizes and spacings of these various features to scale, and to reflect in this sketch the respective abundances appropriate for the indicated wind speed of 10 ms^{-1}.

The most visible category of feature on the sea surface when the winds are well above 4 ms^{-1} is the aerated spilling wave crest or active whitecap (surface feature "A" on Fig. 1), which has a visible albedo of about 0.5 [11], [12]. These Stage A whitecaps also markedly enhance the satellite-sensed average microwave backscattered cross section of the sea surface as a consequence of Bragg scattering [13] and are known to give rise to "sea spikes" on the display of navigational radar sets. These active whitecaps and the concentrated bubble plumes (α of Fig. 1) of which they are the surface expressions have very short characteristic lifetimes [14], persisting for significantly longer than 1 s only when they are episodically renewed by the repetitive pulse-like action of their parent spilling waves.

Another pronounced feature of the sea surface is the mature whitecap or hazy foam patch ("B" of Fig. 1), which is what each Stage A whitecap immediately decays into. These relatively large sea-surface features have an average effective visible reflectance, or albedo, of about 0.2 [15] and greatly enhance the microwave emissivity of the ocean surface [16], [17]. It is this strong influence of whitecap cover-

0364-9059/90/1000-0340$01.00

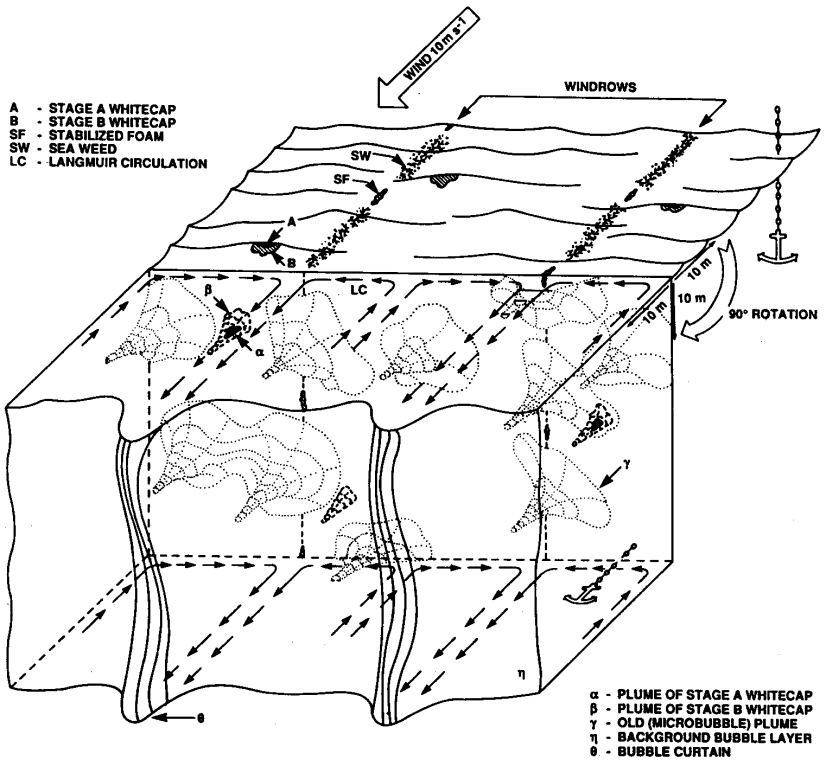

Fig. 1. Stages in the evolution of the bubble plume produced when air is entrained by a spilling wave crest. The influence of Langmuir circulation on these plumes and the background bubble population is also shown in this figure. Note the arrows marking off 10 m along the axes of this scale drawing. (See text for details.)

age on sea-surface microwave emissivity and hence on apparent oceanic brightness temperature that makes feasible the suggestion that it should be possible to routinely monitor regional whitecap coverage with satellite-borne scanning multichannel microwave radiometers [18]. The area of each Stage B whitecap decreases with time in an approximately exponential fashion [19], with an e-folding time of typically 3.5 to 4.3 s [20]. The fraction of the sea surface expected to be covered by Stage B whitecaps when the 10-m elevation wind speed is 10 ms^{-1} is about 0.010 (i.e., close to 1% [21]) when the wind has been blowing long enough to give rise to a fully developed sea.

Other features often encountered when the ocean has been subjected to a protracted steady wind are windrows [7], bands of buoyant material aligned with the wind and marking the surface flow convergence zones associated with the pairs of counter-rotating horizontal vortices that make up the frequently present Langmuir circulation. In addition to being marked by bands of Sargassum [22], [23] ("SW" on Fig. 1), persistent bubbles and stable foam patches ("SF") are often found in windrows. They occur in these bands because oils, of natural or anthropogenic origin, and surfactants are concentrated along these lines of horizontal convergence, and these materials are effective at lowering the surface tension and greatly enhancing the lifetimes of bubbles once they reach the sea surface.

The most visible features to be found immediately beneath a sea surface on which waves are breaking are the aforementioned α-plumes, the subsurface extensions of the Stage A whitecaps. In addition to being quite amenable to detection by investigators using submerged film- or video-cameras, these new plumes are considered to be probable sources of high-frequency sound [2]–[5], with the individual energized bubbles acting as incoherent monopole sound sources. These α-plumes will also greatly influence near-surface sound transmission, having void or air volume fractions estimated to be as great as 8% [24]. Bezzabotnov [25], from photographs taken with a raft-borne camera in the Baltic and Caspian Seas, concluded that right at the surface the void fraction of a Stage A whitecap was approximately 11%, and at a depth of 0.1 m for the associated new plume it ranged up to 3%. Longuet-Higgins and Turner [26] suggest that the void fraction right at the crest of a spilling wave, where the slope of the sea surface is 30°, may be as high as 30%, and point out that a minimum void fraction of 8% is required to maintain a steady spilling whitecap. (It is worth noting in this context that water just as it flows over the sill of a dam has been found to contain 25 to 30% air by volume [27].) These plumes will quickly decay into the β-plumes shown also in Fig. 1. The bubble concentration and the shape of the bubble spectrum are conjectured to still be quite uniform over depth within these β-plumes [10], [20], which are perceived to be

downwardly attenuating columns of aerated water, each of whose horizontal cross sections decreases exponentially with depth [28], [9]. The e-folding depth of these columns is taken to be approximately 0.5 m, consistent with the rate of decrease with depth of the acoustic scattering cross section of bubble clouds as measured with a 248-kHz sonar by [29]. A void fraction of 1 or 2×10^{-4} has been inferred for these β-plumes [24], from a consideration of Johnson and Cooke's [30] measurements of bubbles at a 1.8-m depth for winds of 13 ms^{-1}, and the assumption that essentially all of the bubbles observed by [30] were concentrated within the cross-sectional areas (duly reduced for depth) of the plumes beneath the Stage B whitecaps that would be expected to dot the sea surface under these conditions [21]. It should be noted that Bezzabotnov's [25] several photographic samples taken at a 0.1-m depth of 3 to 4 s-old bubble plumes yielded void fractions in the 1×10^{-3} to 2×10^{-3} range. The bubble aggregate represented by each of these plumes is postulated to act in some fashion as a coherent monopole source of low-frequency sound [4], [5]. These plumes, which are just within the typical contrast resolution limits of the available underwater camera systems, are also readily detected with high-frequency sonars. When a β-plume, which has the same characteristic lifetime or characteristic time scale defining its exponential decay as does a Stage B whitecap, disappears, no visually detectable subsurface bubble-feature remains, with the possible exception of the underside of the stabilized foam patch which might result if the original plume was generated in the immediate vicinity of one of the surface-convergence zones associated with a prevailing Langmuir circulation.

But after the last visual vestige of a spilling wave has disappeared, a large subsurface plume that is still clearly detectable by acoustic means will persist. Ten such γ-plumes are included in Fig. 1. On any occasion, many more γ-plumes than β-plumes will be found in the surface layer of the ocean, since the lifetime of a γ-plume, which typically persists for hundreds of seconds [31], is much longer than the lifetime of a β-plume. Each of the γ-plumes is much larger than the typical β-plume because turbulent diffusion has by this stage spread those bubbles that remain from the original bubble population that formed when the parent wave spilled over a much greater volume of water. The bubble spectrum characterizing a γ-plume is considerably narrower than the spectrum associated with the precursor α- and β-plumes, since enough time has elapsed for most of the larger bubbles to have risen to the surface, and, depending on the levels of dissolved oxygen and nitrogen in the surface waters [29], for some or all of the smaller bubbles to go into solution. Given this loss of the largest and smallest bubbles and the general dilution resulting from the turbulent mixing, the concentration of bubbles in the γ-plume is much less than in the β-plume, and this concentration decreases with depth within each plume. The void fraction within a γ-plume is estimated [24] to be in the range of 10^{-6} to 10^{-7}. While the actual shape of the γ-plumes may vary between columnar and billowy, as described by [29], these plumes are shown in Fig. 1 as narrowing exponentially with increasing depth, reflecting the observation that the scattering cross sections of bubble clouds do show an exponential decrease with depth [29].

After still more time has passed since the genesis of a bubble plume in a spilling wave, the remaining bubbles will be so well mixed, particularly in the horizontal plane, that they will appear as a modest contribution to the background bubble field, which can in most instances be described as a horizontally near-homogeneous bubble population in which the concentration falls off exponentially with depth. A bubble spectrum such as that described by [32] for winds of 11 to 13 ms^{-1} and a depth of 8 m and an associated void fraction of between 10^{-8} and 10^{-9} [24] has been suggested for this background population under these same conditions. If a certain void fraction is chosen arbitrarily as the discriminant defining the bottom of the background bubble layer, then the three-dimensional region labeled η on Fig. 1 can be taken to represent this layer.

Now the actual effective lifetime of the individual γ-plumes will be highly dependent on the concentration of dissolved oxygen and nitrogen in the surface waters, as will the persistence of the background bubble population [29], [33]. It should be noted that Johnson [34] and others have suggested that one component of the background population may be made up of microbubbles that have been stabilized by surface-active materials present in seawater [35], [36]. Even monolayers of nonpolar material, such as quartz particles, have been shown to be effective at mechanically stabilizing microbubbles [37].

While the lifetimes of γ-plumes do vary, they are typically long enough for the individual γ-plume, in the presence of a Langmuir circulation, to be displaced by the flow associated with this cell-like circulation ("LC" in Fig. 1) in such a fashion that the population of γ-plumes is concentrated in the surface convergence zones [38]. In Fig. 1 no less than five of the ten γ-plumes depicted are shown aligned along the two Langmuir surface convergence zones. The Langmuir circulation, when it is present, will also distort the otherwise relatively homogeneous horizontal distribution of bubbles in the background population. Specifically, the down-welling directly under the surface convergence zones will cause vertical curtains, or walls, to form, in which the background bubble population is considerably higher than immediately outside the curtain on either side [39]. Two such bubble curtains, labeled "θ," are shown in Fig. 1.

Recently, evidence supporting the contention that the lifetimes of γ-plumes are highly dependent on the concentration of the major atmospheric gases in solution in the surface layer of the ocean has come from a somewhat unexpected quarter. Specifically, these data were the product of the most recent [40] in a series of laboratory studies [19], [41] of the role of the bubbles formed when a wave breaks in injecting sea-spray droplets into the atmosphere when they rise to the surface and burst [42], [43]. The droplets are trapped within a hood or cover which encloses the whitecap simulation tank, and the concentration or actual number of particles that is generated by a single breaking wave of known size is recorded as a function of time from the moment the wave broke. Two such time traces have been reproduced in Fig. 2. The trace

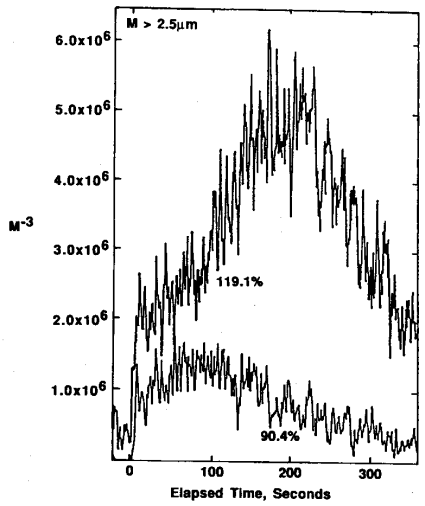

Fig. 2. Concentration of jet-droplets with radii of 25 μm or larger in the hood of a whitecap simulation tank as a function of the time elapsed since a breaking wave event. This is a measure of the cumulative production of jet-droplets by bursting bubbles of 50 μm and larger radius, and as such is an indication of the number of these bubbles that survive to rise to the sea-water surface, for the two indicated dissolved oxygen saturation levels. (See text for details.)

labeled 119.1% was recorded when a wave was caused to break in seawater which was 119.1% saturated with respect to dissolved oxygen. Since the levels of gas saturation in these studies were obtained by quite-rapidly altering the temperature of the seawater in the tank at the University of Connecticut, and since the temperature dependence of nitrogen solubility is near to that of oxygen [44], it can be assumed that the seawater was supersaturated with nitrogen to a like extent. The trace labeled 90.4% was obtained when a wave broke in water that was only 90.4% saturated with dissolved oxygen. Both traces record the concentration of sea-spray droplets with radii greater than 2.5 μm. It is assumed that these are primarily jet-droplets [45], the droplets pinched off the rising Worthington jet formed by the radial inrush of water into the hollow, nearly hemispherical cavity formed by the bursting of the upper surface or film of the protruding bubble [42], [46]. In light of this assumption, and aware that the relative humidity was in the range of 60 to 80%, it can be concluded [42], [47], [48] that these jet droplets were produced from bubbles with a radii of 50 μm or slightly larger.

The time designated "0" on the abscissa of Fig. 2 corresponds to the breaking-wave event. The right-hand ends of both traces on this figure shown a decline in marine aerosol concentration as a consequence of droplet sedimentation or fallout. A comparison of the left-hand rising sections of these two traces strongly suggests that bubbles of about 50-μm radius survived to rise to the surface for fully several hundred seconds after the α-plume was formed in the instance where the seawater was 119.1% saturated with oxygen (and nitrogen), but that these same bubbles only survived for some tens of seconds when the water was only 90.4% saturated.

In this section, an attempt has been made to set forth, by calling on a broad range of optical and acoustic observations, a coherent picture of the life history of a subsurface bubble plume and of its accompanying surface whitecap. It must be acknowledged that this is but a preliminary synthesis of the available observations, and certain specifics included in this development, such as the void fraction or bubble spectrum to be identified with a certain stage of plume evolution, may in fact be incorrect. It is hoped that the simple model of the evolution of a bubble plume illustrated in Fig. 1 will serve as a unifying framework for those interested in developing a more precise understanding of the fate of this plume or, as it is often described [8], bubble cloud produced when a wave breaks at sea.

III. Dependence of Whitecap Coverage on Wind Speed

In the previous section it was stated that for winds of 10 ms^{-1}, approximately 1% of the sea surface will be covered by Stage B whitecaps. An indication of the strong dependence of whitecap coverage on 10-m elevation wind speed is in order. Using the same $W_B(U)$ power-law expression [21], based as it is on a robust bi-weight fit analysis of the East China Sea [49] and BOMEX "plus" [50] whitecap data sets, it can be inferred that if the winds freshen to 20 ms^{-1}, then the fraction of the sea covered by Stage B whitecaps will increase to about 0.105; i.e., to near 10.5%. Such power-law expressions are convenient and have been used in one form or another for at least a quarter century to describe $W_B(U)$ [42], [51], but there are some inherent shortcomings associated with these mathematical descriptions [21], [52].

Recognizing that W_B should be proportional to u_*^3 (i.e., to the cube of the friction velocity) as contended by [51] and [53], and acknowledging the desirability of expressing whitecap coverage in terms of an appropriate nondimensional quantity, in this section the Stage B whitecap data, resulting from the analysis of oblique photographs of the sea surface [54], will be displayed on cartesian plots of $W_B^{1/3}$ versus $U(g\nu)^{-1/3}$, where g is the acceleration due to gravity and ν is the kinematic viscosity of sea water. It should be noted that the kinematic viscosity of sea water varies markedly with water temperature [6]. Henceforth the nondimensional 10-m elevation wind speed $U(g\nu)^{-1/3}$ will be represented by V. In choosing such a presentation, the problem associated with trying to deal in log–log space [21], [51] with the many null whitecap observations that are routinely recorded is avoided. Included within the $W_B^{1/3}$ V-space of Fig. 3 are the individual Stage B whitecap observations from the two data sets already referred to [49], [50], and the additional W_B points obtained from the analysis of the groups of oblique photographs taken of the sea surface west of Scotland and north of Ireland during the JASIN experiment [55]. On this figure each of these three data sets has been described by a straight line in $W_B^{1/3}V$-space, a line fitted by using the technique of ordinary least squares. All of these lines intersect the $W_B^{1/3}$-equals-zero axis at V values between 67 and 113. For a sea water temperature of 21.66°C, the average water temperature associated with the 175 whitecap observations plotted on Fig. 3, these V values correspond to U values between 1.44

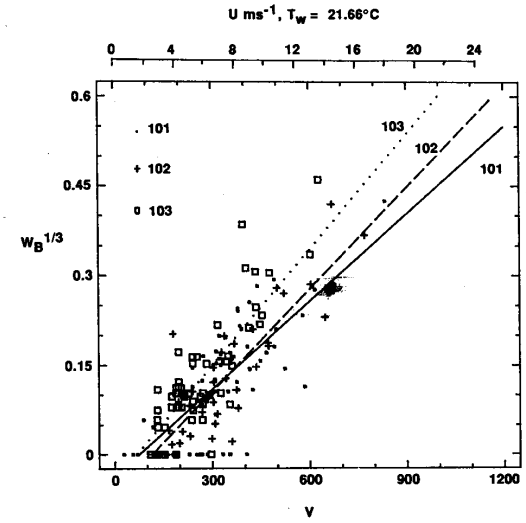

Fig. 3. The cube root of the fraction of the sea surface covered by Stage B whitecaps versus V, the nondimensional wind velocity. V equals $U_{10}(g\nu)^{-1/3}$, where U_{10} is the 10-m elevation wind speed, g is the acceleration due to gravity, and ν is the kinematic viscosity of sea water. 101 = Whitecap observations from BOMEX "plus" [43]. 102 = Observations from the East China Sea [42]. 103 = Observations from the JASIN experiment [48]. Note the auxiliary abscissa, which gives U_{10} for the average sea-water temperature determined for the 175 observations that make up the three data sets. Each line is a result of fit by linear regression in $W_B^{1/3}$, V space to the indicated data set.

and 2.43 ms^{-1}. (For convenience, a U scale appropriate for a T_W of 21.66°C has been added to this figure.) It is of interest to note that these values for the wind speed at which whitecaps first appear, a speed sometimes referred to as U_B, the Beaufort velocity, are somewhat below the 2.88 ms^{-1} value for U_B predicted for this T_W by [6, equation (2)], an expression arrived at by an entirely different approach. According to the whitecap/bubble-plume model described in Section II, the onset of whitecapping is coincident with the initiation of bubble-plume formation. Thus it is relevant to record that the wind speed at which the penetration depth of bubble clouds shrinks to zero, as deduced from the Loch Ness sonagraph records obtained by [56], is 2.5 ms^{-1}, a speed quite consistent with the aforementioned values for U_B. Subsequent acoustic observations made by Thorpe at a coastal site near Oban, Scotland [29], in the Irish Sea [31], and on the edge of the European continental shelf [31] are consistent with 2.5 ms^{-1} being the wind speed associated with the advent of bubbles in the water column.

It has long been recognized that, aside from the 10-m elevation wind speed, the thermal stability of the lower atmosphere will greatly influence the fractional whitecap coverage of the ocean surface [54], [57]. While the influence of changes in T_W on W_B, thought to result primarily from the T_W dependence of the kinematic viscosity [6], has been accommodated in the manner in which U has been nondimensionalized to yield V, the effect of atmospheric thermal stability on W_B still needs to be taken into account. It is reasonable to contend that, for a given wind duration and fetch, the sea state, the frequency of wave breaking, and the fractional whitecap coverage should be more closely related to the wind stress upon the sea surface τ, or to the product of τ and the surface drift current [53], than to the 10-m elevation wind speed U. The foregoing suggests that $W_B^{1/3}$ should be parameterized in the first instance in terms of the friction velocity u^*, which is defined in terms of the wind stress and air density ρ_A as follows [58]:

$$u^* = (\tau/\rho_A)^{1/2}. \tag{1}$$

(The actual procedure selected in the present study to calculate u^* from U, T_W, and the deck-height air temperature T_A is that given by [59]. More detailed descriptions of the relationship between U, u^* and the various other properties of the lower marine atmospheric boundary layer can be found in [60] and [58].) Having obtained a u^* value for each measured U, a nondimensional u^* value calculated from $u^*(g\nu)^{-1/3}$ and designated v^* was then determined for each whitecap observation interval. The same three whitecap data sets as were plotted on Fig. 3 have been replotted in $W_B^{1/3}v^*$-space on Fig. 4.

White the various photographic whitecap data sets collected by Western and Japanese investigators have been "manually" analyzed [54] only for W_B-values, several Soviet researchers have analyzed photographs of the sea surface to obtain W_A and W_B values from the same photographic images [61], [62]. Recently, video recordings of oblique views of the ocean surface have been analyzed using a Hamamatsu Area Analyzer, and the resulting fractional whitecap coverage values have been shown to be in rough agreement with the W_A values obtained for the same wind speeds by the Soviet investigators [20]. In Fig. 5(a) are to be found the 322 measurements of the fraction of the sea surface covered by spilling wave crests (i.e., by Stage A whitecaps) obtained from the analysis of the oblique video images recorded during the MIZEX 83 [63], MIZEX 84 [64], HEXPILOT [63], and HEXMAX [65] field programs plotted in $W_A^{1/3}V$-space. Also in Fig. 5(a) are plotted in the 350 W_B values obtained from the analysis of six sets of whitecap photographs, the three sets previously described plus the sets of photographs collected during the STREX [66], MIZEX 83 [67], and MIZEX 84 [64] field experiments.

The straight line obtained by ordinary least-squares fitting to describe $W_A^{1/3}(V)$ intersects the abscissa of Fig. 5 at a V value of 104, while the comparable line describing $W_B^{1/3}(V)$ intersects the horizontal axis at $V = 75.8$. For the average seawater temperature determined for these 672 W_A and W_B observations (i.e., for 11.10°C), these intersections correspond to Beaufort velocities of 2.43 and 1.77 ms^{-1}, respectively. The same W_A and W_B observations have been replotted in $W_{A/B}^{1/3}$, v^* space in Fig. 5(b).

While Fig. 5(a) and (b) looks quite similar, it should be noted that the correlation coefficient determined for the $W_A^{1/3}(V)$ line is somewhat higher (0.767) than that for the $W_A^{1/3}(v^*)$ line (0.739), and likewise the correlation coefficient associated with the $W_B^{1/3}(V)$ line is higher (0.766) than the equivalent measure for the $W_B^{1/3}(v^*)$ line (0.689). At first consideration, this might be taken as an indication that V is a more suitable parameterization for W_B and W_A than v^*,

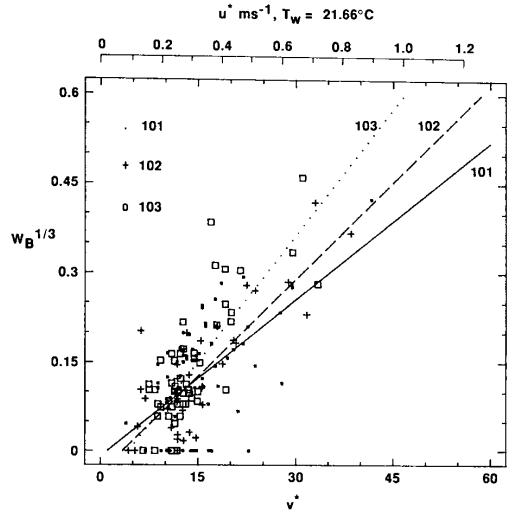

Fig. 4. The cube root of the fraction of the sea surface covered by Stage B whitecaps versus v^*, the nondimensional friction velocity. v^* equals $u^*(g\nu)^{-1/3}$, where u^* is the friction velocity. See the caption of Fig. 3 for the designation of data sets 101, 102, and 103.

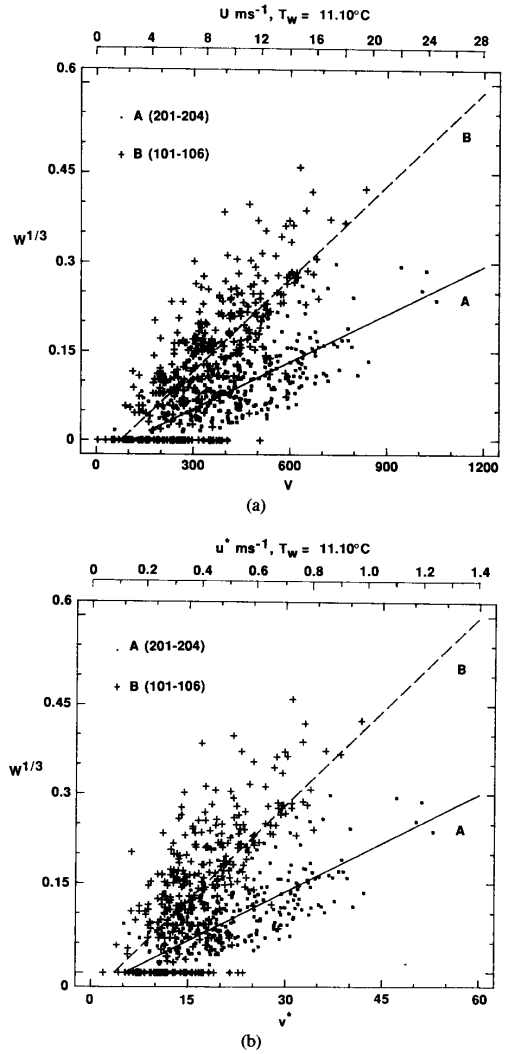

Fig. 5. (a) The cube root of the fraction of the sea surface covered by whitecaps versus V, the nondimensional wind velocity. (b) The cube root of the fraction of the sea surface covered by whitecaps versus v^*, the nondimensional friction velocity. Line A: Fit in $W_A^{1/3}$, V-, or $W_A^{1/3}$, v^*-, space to Stage A whitecap data sets from MIZEX 83 [55], MIZEX 84 [56], HEXPILOT [55], and HEXMAX [57] field programs. Line B: Fit in $W_B^{1/3}$, V-, or $W_B^{1/3}$-, v^*-, space to stage B whitecap data sets from BOMEX "plus" [43], East China Sea [42], JASIN [48], STREX [58], MIZEX 83 [59], and MIZEX 84 [56] field programs. The two auxiliary abscissa give corresponding U_{10} and u^* values for the average sea-water temperature determined for the 672 W_A and W_B observations that make up these ten (201-204, 101-106) data sets.

contrary to the suggestion that appeared earlier in this section. But, in reality, the lower correlation coefficients associated with the straight lines in $W_{A/B}^{1/3}v^*$ space are probably a consequence of the fact that all of the W_A data sets, and most of the W_B data sets, were collected in regions of the world ocean where the high wind-speed episodes where often of insufficient duration to generate fully developed seas. As has been shown by [6] in an earlier analysis, in $\ln W_B, \ln U$ space, of the first five of the W_B data sets discussed in this paper, the bias introduced by the high wind but less-than-fully developed sea observations results in a reduced apparent wind dependence of W_B. Specifically, they found that for these five data sets, W_B was proportional to $U^{2.55}$. Now such a combined data set is not as amenable to description by a straight line in $W_B^{1/3}$, U, or $W_B^{1/3}$, V space as a data set in which W_B is proportional to U^3. It should here be noted that the drag coefficient introduced in the present study into Smith's [59] expression for calculating u^* from U, T_W, and T_A manifests a slight positive linear dependence on U, consistent with the findings of various boundary-layer investigations [68]-[70]. Thus the u^* or v^* dependence of W_B can be expected to be even less than that reflected in the 2.55 power-law mentioned above, and the attempt to describe the W_B, u^*, or W_B, v^* data by a straight line in $W_B^{1/3}, u^*$ or $W_B^{1/3}, v^*$ space is even less successful than the attempt in $W_B^{1/3}, U$ or $W_B^{1/3}, V$ space. This same rationale applies when considering the goodness-of-fit of straight lines to the $W_A^{1/3}, V$ and $W_A^{1/3}, v^*$ points.

The clustering of $W_A^{1/3}, v^*$ and $W_B^{1/3}, v^*$ points along straight lines may be more pronounced when whitecap observations become available, for which the associated wind stress or v^* values were obtained by the direct Reynolds eddy correlation or dissipation methods [71], as opposed to being inferred from bulk formulae involving U, T_W, and T_A.

The amplitude of the $W_B^{1/3}$ line in Fig. 5 is slightly more than twice the amplitude of the $W_A^{1/3}$ line for the same value of V or v^*, indicating that for a particular wind speed or sea state, the fraction of the sea surface covered at any instant by mature Stage B whitecaps is about nine or ten times the fraction covered by Stage A spilling crests. This result is consistent with the relative sizes of the tops of the β- and α-plumes depicted in Fig. 1 and with the relative effective lifetimes of the individual Stage B and Stage A whitecaps.

IV. Discussion

The rate of formation of the new whitecap surface area can be inferred from estimates of W_A or W_B [50], quantities which can in turn be estimated from satellite measurements of the sea-surface microwave backscatter cross section and the sea-surface apparent microwave brightness temperature, respectively. The rate of bubble injection can therefore be deduced from measurements of W_A or W_B [9], and if the effective terminal rise velocity of air bubbles in seawater is known, then the concentration and size spectrum of the bubble population just beneath the sea surface can likewise be estimated from W_A or W_B [10].

Working backwards from the models relating sea-surface aerosol flux to W_B [28], [41], the expression given in (2) was obtained for $\partial C/\partial R$, the number of bubbles per cubic meter of seawater per micrometer increment in bubble radius [9], [10]. It should be noted that in restating this equation, account has been taken of the fact that the radius of an aerosol droplet at 80% relative humidity (RH), the RH for which the aerosol flux equations apply, is 0.5 the radius of that same droplet at the instant it was produced at the end of the Worthington Jet formed when the parent bubble collapsed, and that according to [42], the radius of this droplet at the moment of its formation r is related to the parent bubble radius R by the expression, $r = 8.77 \times 10^{-2}R + 0.98$. Strictly speaking, this relationship between r and R applies solely to the top droplet formed from such a jet. But since it appears that the second droplet from a jet is only some 8–12% larger than would be deduced from this equation [72], and the next several droplets some 20% smaller [73], it seems quite in order to use this $r(R)$ expression in the present calculations. In (2), $v_T(R)$ represents the terminal rise velocity of a bubble of radius R:

$$\partial C/\partial R = \left[v_T(R)\,J\right]^{-1}(1 - 0.845e^{-0.015R}) \times 1.56 \times 10^4 \times (4.38 \times 10^{-2}R + 0.49)^{-3} \times \left[1 + 0.057(4.38 \times 10^{-2}R + 0.49)^{1.05}\right] \times 10^{1.19e^{-y^2}} W_B \quad (2)$$

where $Y = [0.380 - \mathrm{LOG}_{10}(4.38 \times 10^{-2}R + 0.49)]/0.650$, and J stands for the number of jet-droplets found to be produced per bursting bubble. The extent to which the resident bubble spectrum predicted by (2), when W_B is assumed to be 0.0241, i.e., when U is taken to be 13 ms^{-1}, agrees with the near-surface bubble spectra observed at sea under comparable wind conditions by [32] and [30] and with the fresh-water bubble spectrum measured by [74] in a wind-wave flume for an equivalent sea state is described in detail elsewhere [10].

The terminal rise velocity of a bubble of a certain radius will vary markedly depending upon whether the bubble is hydrodynamically clean or dirty [29]. From a consideration of the laboratory findings of [75], it seems appropriate to assume that most of the bubbles in a plume in natural seawater will behave as if they are dirty; i.e., that they will rise through the water column at speeds appropriate for solid spheres of the same radii. Equation (3) was obtained by approximating the terminal rise velocity curve for dirty bubbles shown in [29, fig. 16] with a simple polynomial expression in R, valid to within 4% for R equal to or greater than 25 μm:

$$v_T(\mathrm{ms}^{-1}) = 9.0 \times 10^{1}R^{-3} - 1.5 \times 10^{-1}R^{-1} - 3.5 \times 10^{-3} + 2.35 \times 10^{-4}R - 1.97 \times 10^{-7}R^2. \quad (3)$$

J will be assumed to have a value in the range of 1 to 5, the latter being the number of jet droplets per bubble assumed by [76]. The substitution of (3) for $v_T(R)$ in (2) leads to,

$$\partial C/\partial R = J^{-1}(5.76 \times 10^{-3}R^{-3} - 9.60 \times 10^{-6}R^{-1} - 2.24 \times 10^{-7} + 1.51 \times 10^{-8}R - 1.26 \times 10^{-11}R^2)^{-1}(4.38 \times 10^{-2}R + 0.49)^{-3} \times \left[1 + 0.057(4.38 \times 10^{-2}R + 0.49)^{1.05}\right] \times 10^{1.19e^{-y^2}} W_B \quad (4)$$

where $Y = [0.380 - \mathrm{LOG}_{10}(4.38 \times 10^{-2}R + 0.49)]/0.650$.

Assuming further that (5), the expression recently arrived at by [40], [77] to describe the effect on jet droplet production of the saturation level of the oceanic mixed layer,

$$S(s) = 9.10 \times 10^{-3}e^{+0.0470s} \quad (5)$$

where s is the percentage oxygen (and nitrogen) saturation of the sea water with respect to the major atmospheric gases, can likewise be taken as a relative measure of the fraction of air bubbles which survives to reach the sea surface for a given saturation level, then (6), which was obtained by multiplying (4) by (5), should be an improved expression for the estimation of the concentration of air bubbles, per increment bubble radius, just beneath the sea surface:

$$\partial C/\partial R = J^{-1}(6.33 \times 10^{-1}R^{-3} - 1.06 \times 10^{-3}R^{-1} - 2.46 \times 10^{-5} + 1.66 \times 10^{-6}R - 1.38 \times 10^{-9}R^2)^{-1} \times e^{+0.0470s}(1 - 0.845e^{-0.015R}) \times (4.38 \times 10^{-2}R + 0.49)^{-3} \times \left[1 + 0.057(4.38 \times 10^{-2}R + 0.49)^{1.05}\right] \times 10^{1.19e^{-y^2}} W_B \quad (6)$$

where $Y = [0.380 - \mathrm{LOG}_{10}(4.38 \times 10^{-2}R + 0.49)]/0.650$.

As was observed previously and as can be seen from Fig. 5, the ratio of $W_B^{1/3}$ to $W_A^{1/3}$ for a given value of V is slightly greater than 2:1. Taking 2.13 as a typical value for this ratio, (6) can be recast in terms of W_A by making the simple substitution of 9.7 W_A for W_B. Likewise, if no direct estimate of either W_B or W_A is available but if values for U and T_W have been recorded so that V can be determined,

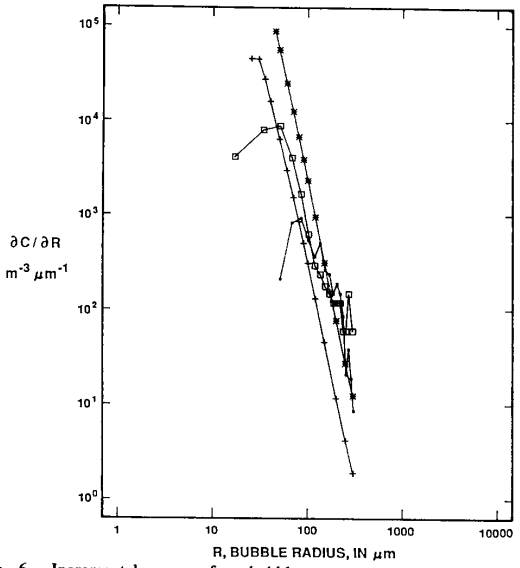

Fig. 6. Incremental near-surface bubble concentration, $\partial C/\partial R$, versus bubble radius R. Crosses, model described by equation (6), for $J = 5$, $s = 100\%$, $U_{10} = 13$ ms^{-1}, and $T_W = 19.9$°C. Asterisks, same model evaluated for $J = 1$, $s = 105\%$, $U_{10} = 13$ ms^{-1}, and $T_W = 19.9$°C. Filled squares, data from run "Kimbla No. 3" of Walsh and Mulhearn [78] for which U_{10} was 13 ms^{-1}, T_W was 19.9°C, and the camera depth was 1.2 m. Open squares, observations of Johnson and Cooke [24] taken at depth of 0.7 m, when U_{10} was 11-13 ms^{-1} and T_W was 3°C.

then W_B can be calculated from (7), the expression describing the $W_B^{1/3}$ regression line

$$W_B^{1/3} = 5.21 \times 10^{-4}(V - 75.9), \qquad V \geq 75.9 \quad (7)$$

in the upper panel of Fig. 5 and substituted into (6).

As a test of this revised model of the near-surface bubble population, (6) and (7) have been employed to calculate the expected near-surface bubble spectra for a wind speed of 13 ms^{-1}, a surface water temperature of 19.9°C, gas saturation levels of 100 and 105%, and J ranging in value from 1 to 5. These two bubble spectra have been plotted on Fig. 6, along with the spectrum determined by [78] from photographs taken at a depth of 1.2 m when the measured wind speed and water temperature corresponded to the values used in calculating these particular model spectra. (These observations were designated in [78] as HMAS *Kimbla* Run No. 3.) Also plotted on this same figure is the resident bubble spectrum obtained by [30] from photographs taken 0.7-m beneath the sea surface when the winds were 11-13 ms^{-1} and the water temperature was a relatively cold 3°C. While there are some discrepancies between the model and observations for the smaller bubble sizes, discrepancies that may in part be attributed to the limited optical resolution of the camera systems, the degree of agreement between model and field observations in the large bubble range is such as to encourage the further development of the predictive model described by (6).

It is appropriate to note that if (8), the equation describing the $W_B^{1/3}$ line in Fig. 5(b), is combined

$$W_B = 1.19 \times 10^{-6}(v^* - 3.57)^3, \qquad v^* \geq 3.57 \quad (8)$$

with (6), then it becomes explicit that $\partial C/\partial R$ is proportional to $(v^* - 3.57)^3$, i.e., that for all but the smallest values of the nondimensional friction velocity v^*, $\partial C/\partial R$ is essentially proportional to v^{*3}. This is consistent with the prediction of the model of [79] that the near-surface number density of bubbles should vary with the cube of the friction velocity, and in accordance with the conclusions reached by [80] from an analysis of acoustic measurements made in Queen Charlotte Sound, British Columbia, as it was likewise deduced that the population densities of bubbles of 132 and 229-μm radius, for wind speeds in the 10 to 16 ms^{-1} range, varied as u^{*3}.

Acknowledgment

The selection of $W^{1/3}$ and $U(g\nu)^{-1/3}$ as coordinates for the presentation of whitecap data owes much to the helpful suggestions made to ECM by Prof. H. Charnock of the University of Southampton (UK), and by Prof. L. Hasse of the Institut für Meereskunde, Kiel (FRG). The insights provided by Prof. I. G. O'Muircheartaigh of University College, Galway (Ireland) are gratefully acknowledged, as is the invaluable assistance rendered by M.B. Wilson and E. J. Minik of the University of Connecticut.

References

[1] H. Medwin, "Acoustic fluctuations due to microbubbles in the near-surface ocean," *J. Acoust. Soc. Amer.*, vol. 56, pp. 1100-1104, 1974.

[2] P. A. Crowther, "Bubble noise creation mechanisms," in *Sea Surface Sound*, B. R. Kerman, Ed. Dordrecht: Kluwer Academic, 1988, pp. 131-150.

[3] M. L. Banner and D. H. Cato, "Physical mechanisms of noise generation by breaking waves—a laboratory study," in *Sea Surface Sound*, B. R. Kerman, Ed. Dordrecht: Kluwer Academic, 1988, pp. 429-436.

[4] A. Prosperetti, "Bubble dynamics in oceanic ambient noise," in *Sea Surface Sound*, B. R. Kerman, Ed. Dordrecht: Kluwer Academic, 1988, pp. 151-171.

[5] W. M. Carey and D. Browning, "Low frequency ocean ambient noise: Measurements and theory," in *Sea Surface Sound*, B. R. Kerman, Ed. Dordrecht: Kluwer Academic, 1988, pp. 361-376.

[6] E. C. Monahan and I. G. O'Muircheartaigh, "Whitecaps and the passive remote sensing of the ocean surface," *Int. J. Remote Sensing*, vol. 7, pp. 627-642, 1986.

[7] S. A. Thorpe, "Small-scale processes in the upper ocean boundary layer," *Nature*, vol. 318, pp. 519-522, 1985.

[8] S. A. Thorpe, "The horizontal structure and distribution of bubble clouds," in *Sea Surface Sound*, B. R. Kerman, Ed. Dordrecht: Kluwer Academic, 1988, pp. 173-183.

[9] E. C. Monahan, "Whitecap coverage as a remotely monitorable indication of the rate of bubble injection into the ocean mixed layer," in *Sea Surface Sound*, B. R. Kerman, Ed. Dordrecht: Kluwer Academic, 1988, pp. 85-96.

[10] E. C. Monahan, "Near-surface bubble concentration and oceanic whitecap coverage," in *Proc. 7th Conf. Ocean-Atmos. Interaction* (Anaheim, CA). Boston: Amer. Meteorol. Soc., 1988, pp. 178-181.

[11] C. H. Whitlock, D. S. Bartlett, and E. A. Gurganus, "Sea foam reflectance and influence on optimum wave-length for remote sensing of ocean aerosols," *Geophys. Res. Lett.*, vol. 9, pp. 719-722, 1982.

[12] P. J. Stabeno and E. C. Monahan, "The influence of whitecaps on the albedo of the sea surface," in *Oceanic Whitecaps and Their Role in Air-Sea Exchange Processes*, E. C. Monahan and G. MacNiocaill, Eds. Dordrecht: Reidel, 1986, pp. 261-266.

[13] M. L. Banner and E. H. Fooks, "On the microwave reflectivity of small-scale breaking water waves," *Proc. Roy. Soc. London*, vol. A399, pp. 93-109, 1985.

[14] M. Donelan, M. S. Longuet-Higgins, and J. S. Turner, "Periodicity in whitecaps," *Nature*, vol. 239, pp. 449-451, 1972.

[15] P. Koepke, "Oceanic whitecaps: Their effective reflectance," in *Oceanic Whitecaps and Their Role in Air-Sea Exchange Processes*, E. C. Monahan and G. MacNiocaill, Eds. Dordrecht: Reidel, 1986, pp. 272-274.
[16] J. D. Droppleman, "Apparent microwave emissivity of sea foam," *J. Geophys. Res.*, vol. 75, pp. 696-698, 1970.
[17] G. F. Williams, Jr., "Microwave radiometry of the ocean and the possibility of marine wind velocity determination from satellite observations," *J. Geophys. Res.*, vol. 74, pp. 4591-4594, 1969.
[18] P. Gloersen and F. T. Barath, "A scanning multichannel microwave radiometer for Nimbus-G and Seasat-A," *IEEE J. Oceanic Eng.*, vol. OE-2, pp. 172-178, 1977.
[19] E. C. Monahan, K. L. Davidson, and D. E. Spiel, "Whitecap aerosol productivity deduced from simulation tank measurements," *J. Geophys. Res.*, vol. 87, pp. 8898-8904, 1982.
[20] E. C. Monahan, "From the laboratory tank to the global ocean," in *Climate and Health Implications of Bubble-Mediated Sea-Air Exchange*, E. C. Monahan and M. A. Van Patten, Eds. Groton, CT: CT Sea Grant College Program, 1989, pp. 43-63.
[21] E. C. Monahan and I. G. O'Muircheartaigh, "Optimal power-law description of oceanic whitecap coverage dependence on wind speed," *J. Phys. Oceanogr.*, vol. 10, pp. 2094-2099, 1980.
[22] I. Langmuir, "Surface water motion induced by wind," *Science*, vol. 87, pp. 119-123, 1938.
[23] A. H. Woodcock, "A theory of surface water motion deduced from the wind-induced motion of the *Physalia*," *J. Marine Res.*, vol. 5, pp. 196-205, 1944.
[24] E. C. Monahan, J. P. Kim, M. B. Wilson, and D. K. Woolf, "Oceanic whitecaps and the marine microlayer spanning the boundary separating the sub-surface bubble clouds from the aerosol laden marine atmosphere," Univ. of Connecticut, Avery Point, Whitecap Rep. No. 3, pp. 1-108, 1987.
[25] V. Z. Bezzabotnov, "Some results on the changes of the structure of sea foam formations in the field," *Fiz. Atmosfery i Okeana*, vol. 21, pp. 101-104, 1985 (in Russian).
[26] M. S. Longuet-Higgins and J. S. Turner, "An 'entrained plume' model of a spilling breaker," *J. Fluid Mech.*, vol. 63, pp. 1-20, 1974.
[27] T. S. Artyukhina, "Surface oscillations in a jet falling from a cylindrical crest sill (on a dam)," *Fluid Mech.—Sov. Res.*, vol. 5, pp. 67-75, 1976.
[28] E. C. Monahan, "The ocean as a source for atmospheric particles," in *The Role of Air-Sea Exchange in Geochemical Cycling*, P. Buat-Menard, Ed. Dordrecht: Reidel, 1986, pp. 129-163.
[29] S. A. Thorpe, "On the clouds of bubbles formed by breaking wind-waves in deep water, and their role in air-sea gas transfer," *Phil. Trans. Roy. Soc. London*, vol. A304, pp. 155-210, 1982.
[30] B. Johnson and R. C. Cooke, "Bubble populations and spectra in coastal waters: A photographic approach," *J. Geophys. Res.*, vol. 84, pp. 3761-3766, 1979.
[31] S. A. Thorpe, "Measurements with an automatically recording inverted echo sounder; ARIES and the bubble clouds," *J. Phys. Oceanogr.*, vol. 16, pp. 1462-1478, 1986.
[32] P. A. Kolovayev, "Investigation of the concentration and statistical size distribution of wind-produced bubbles in the near-surface ocean layer," *Oceanology*, vol. 15, pp. 659-661, 1976.
[33] S. A. Thorpe, "The role of bubbles produced by breaking waves in super-saturating the near-surface ocean mixing layer with oxygen," *Ann. Geophys.*, vol. 2, pp. 53-56, 1984.
[34] B. D. Johnson, "Bubble populations: Background and breaking waves," in *Oceanic Whitecaps and Their Role in Air-Sea Exchange Processes*, E. C. Monahan and G. MacNiocaill, Eds. Dordrecht: Reidel, 1986, pp. 69-73.
[35] B. D. Johnson and R. C. Cooke, "Generation of stabilized microbubbles in seawater," *Science*, vol. 213, pp. 209-211, 1981.
[36] P. J. Mulhearn, "Distribution of microbubbles in coastal waters," *J. Geophys. Res.*, vol. 86, pp. 6429-6434, 1981.
[37] B. D. Johnson and P. J. Wangersky, "Microbubbles: Stabilization by monolayers of adsorbed particles," *J. Geophys. Res.*, vol. 92, pp. 14 641-14 647, 1987.
[38] S. A. Thorpe and A. J. Hall, "The characteristics of breaking waves, bubble clouds, and near-surface currents observed using side-scan sonar," *Continental Shelf Res.*, vol. 1, pp. 353-384, 1983.
[39] S. A. Thorpe, "The effect of Langmuir circulation on the distribution of submerged bubbles caused by breaking wind waves," *J. Fluid Mech.*, vol. 142, pp. 151-170, 1984.
[40] M. Stramska, R. Marks, and E. C. Monahan, "Bubble-mediated aerosol production as a consequence of wave breaking in supersaturated (hyperoxic) sea-water," *J. Geophys. Res.*, to be published.
[41] E. C. Monahan, D. E. Spiel, and K. L. Davidson, "A model of marine aerosol generation via whitecaps and wave disruption," in *Oceanic Whitecaps and Their Role in Air-Sea Exchange Processes*, E. C. Monahan and G. MacNiocaill, Eds. Dordrecht: Reidel, 1986, pp. 167-174.
[42] D. C. Blanchard, "The electrification of the atmosphere by particles from bubbles in the sea," *Prog. Oceanogr.*, vol. 1, pp. 71-202, 1963.
[43] D. C. Blanchard, "Bacteria and other materials in drops from bursting bubbles," in *Climate and Health Implications of Bubble-Mediated Sea-Air Exchange*, E. C. Monahan and M. A. Van Patten, Eds. Groton, CT: CT Sea Grant College Program, 1989, pp. 1-16.
[44] D. R. Kester, "Dissolved gases other than CO_2," in *Chemical Oceanography, Vol. 1*, 2nd ed., J. P. Riley and G. Skirrow, Eds. London: Academic, 1975, pp. 498-556.
[45] D. K. Woolf, P. A. Bowyer, and E. C. Monahan, "Discriminating between the film-drops and jet-drops produced by a simulated whitecap," *J. Geophys. Res.*, vol. 92, pp. 5142-5150, 1987.
[46] F. MacIntyre, "Flow patterns in breaking bubbles," *J. Geophys. Res.*, vol. 77, pp. 5211-5228, 1972.
[47] S. Hayami and Y. Toba, "Drop production by bursting of air bubbles on the sea surface; (1) experiments at still sea water surface," *J. Oceanogr. Soc., Japan*, vol. 14, pp. 145-150, 1958.
[48] J. W. Fitzgerald, "Approximation formulas for the equilibrium size of an aerosol particle as a function of its dry size and composition and the ambient relative humidity," *J. Appl. Meteorol.*, vol. 14, pp. 1044-1049, 1975.
[49] Y. Toba and M. Chaen, "Quantitative expression of the breaking of wind waves on the sea surface," *Rec. Oceanogr. Works Japan*, vol. 12, pp. 1-11, 1973.
[50] E. C. Monahan, "Oceanic whitecaps," *J. Phys. Oceanogr.*, vol. 1, pp. 139-144, 1971.
[51] J. Wu, "Spray in the atmospheric surface layer: Review and analysis of laboratory and oceanic results," *J. Geophys. Res.*, vol. 84, pp. 1693-1704, 1979.
[52] E. C. Monahan and D. K. Woolf, "Comments on 'Variations of whitecap coverage with wind stress and water temperature,'" *J. Phys. Oceanogr.*, vol. 19, pp. 706-709, 1989.
[53] J. Wu, "Variations of whitecap coverage with wind stress and water temperature," *J. Phys. Oceanogr.*, vol. 18, pp. 1448-1453, 1988.
[54] E. C. Monahan, "Fresh water whitecaps," *J. Atmos. Sci.*, vol. 26, pp. 1026-1029, 1969.
[55] E. C. Monahan, I. G. O'Muircheartaigh, and M. P. Fitzgerald, "Determination of surface wind speed from remotely measured whitecap coverage: A feasibility assessment," in *Proc. EARSeL-ESA Symp. Appl. Remote Sensing Data on the Continental Shelf* (Voss, Norway), 19-20 May 1981, European Space Agency, SP-167, pp. 103-109.
[56] S. A. Thorpe and A. R. Stubbs, "Bubbles in a freshwater lake," *Nature*, vol. 279, pp. 403-405, 1979.
[57] J. Wu, "Oceanic whitecaps and sea state," *J. Phys. Oceanogr.*, vol. 9, pp. 1064-1068, 1979.
[58] H. U. Roll, *Physics of the Marine Atmosphere*. New York: Academic, 1965, 426 pp.
[59] S. D. Smith, "Coefficients for sea-surface wind stress and heat exchange," Bedford Inst. Oceanogr., Dartmouth, NS, Can., pp. 1-31, 1981.
[60] E. L. Deacon and E. K. Webb, "Small-scale interactions," in *The Sea, Vol. 1*, M. N. Hill, Ed. New York: Wiley, 1962, pp. 43-87.
[61] V. G. Bondur and E. A. Sharkov, "Statistical properties of whitecaps on a rough sea," *Oceanology*, vol. 1, pp. 274-279, 1982.
[62] R. S. Bortkovskii, *Air-Sea Exchange of Heat and Moisture During Storms*. Dordrecht: Reidel, 1987, pp. 1-194.
[63] E. C. Monahan, P. A. Bowyer, D. B. Doyle, M. R. Higgins, and D. K. Woolf, "Whitecaps and the marine atmosphere," Univ. College, Galway, Ireland, Rep. No. 8, pp. 1-124.
[64] E. C. Monahan and D. K. Woolf, "Oceanic whitecaps, their contribution to air-sea exchange, and their influence on the MABL," Univ. of Connecticut, Avery Point, Whitecap Rep. No. 1, 1986, pp. 1-135.
[65] E. C. Monahan, M. B. Wilson, and D. K. Woolf, "HEXMAX whitecap climatology: Foam crest coverage in the North Sea, 16 October-23 November 1986," in *Proc. NATO Advanced Workshop, Humidity Exchange Over the Sea Main Experiment*

(*HEXMAX*), *Analysis and Interpretation*, 1988, Univ. of Washington, Seattle, Tech. Rep., W. A. Oost, S. D. Smith, and K. B. Katsaros, Eds., pp. 105-115.
[66] D. M. Doyle, "Marine aerosol research in the Gulf of Alaska and on the Irish West Coast (Inishmore)," M.Sc. thesis, Nat. Univ. of Ireland, 1984.
[67] E. C. Monahan, M. C. Spillane, P. A. Bowyer, M. R. Higgins, and P. J. Stabeno, "Whitecaps and the marine atmosphere," Univ. College, Galway, Ireland, Rep. No. 7, 1984, pp. 1-103.
[68] J. R. Garratt, "Review of drag coefficients over oceans and continents," *Monthly Weather Rev.*, vol. 105, pp. 915-929, 1977.
[69] O. M. Phillips, *The Dynamics of the Upper Ocean*, 2nd ed. Cambridge, UK: Cambridge Univ. Press, 1977, pp. 1-336.
[70] E. L. Deacon and E. K. Webb, "Small-scale interactions," in *The Sea, Vol. 1*, M. N. Hill, Ed. New York: Wiley, 1962, pp. 43-87.
[71] W. G. Large and S. Pond, "Open ocean momentum flux measurements in moderate to strong winds," *J. Phys. Oceanogr.*, vol. 11, pp. 324-336, 1981.
[72] D. C. Blanchard, "The size and height to which jet drops are ejected from bursting bubbles in seawater," *J. Geophys. Res.*, vol. 94, pp. 10 999-11 002, 1989.
[73] D. C. Blanchard and L. D. Syzdek, "Electrostatic collection of jet and film drops," *Limnol. Oceanogr.*, vol. 20, pp. 762-774, 1975.
[74] S. Baldy and M. Bourguel, "Measurements of bubbles in a stationary field of breaking waves by a laser-based single-particle scattering technique," *J. Geophys. Res.*, vol. 90, pp. 1037-1047, 1985.
[75] A. Detwiler and D. C. Blanchard, "Aging and bursting bubbles in trace-contaminated water," *Chem. Eng. Sci.*, vol. 33, pp. 9-13, 1978.
[76] R. J. Cipriano and D. C. Blanchard, "Bubble and aerosol spectra produced by a laboratory 'Breaking Wave,'" *J. Geophys. Res.*, vol. 86, pp. 8085-8092, 1981.
[77] E. C. Monahan *et al.*, "The significance of oceanic whitecaps for various physical processes at the air-sea interface," Univ. of Connecticut, Avery Point, Whitecap. Rep. No. 6, 1989, pp. 1-118.
[78] A. L. Walsh and P. J. Mulhearn, "Photographic measurements of bubble populations from breaking wind waves at sea," *J. Geophys. Res.*, vol. 92, pp. 14 553-14 565, 1987.
[79] B. R. Kerman, "Distribution of bubbles near the ocean surface," *Atmos.-Ocean*, vol. 24, pp. 169-188, 1986.
[80] D. M. Farmer and D. D. Lemon, "The influence of bubbles on ambient noise in the ocean at high wind speeds," *J. Phys. Oceanogr.*, vol. 14, pp. 1762-1778, 1984.

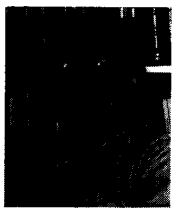

Edward C. Monahan graduated from the five-year engineering physics program at Cornell University, Ithaca, NY (1959), and earned the M.A. (physics) degree from the University of Texas at Austin (1961). He was awarded the Ph.D. degree (oceanography) by the Massachusetts Institute of Technology, Cambridge (1966). In 1984 he received the D.Sc. degree from the National University of Ireland, based on a portfolio of some 30 published works.

He is a Professor of Marine Sciences at the University of Connecticut, and Director of the Connecticut Sea Grant College Program. Prior to that, he taught at a number of other universities, including the University of Michigan and University College, Galway. His primary research interest is in bubble-mediated air-sea exchange processes. Working closely with Professor I. G. O'Muircheartaigh of UCG and others, he has investigated the influence of wind speed and other meteorological and oceanographic factors on the frequency of wave breaking and whitecap formation. He and his colleagues in the Sea Surface Physics Laboratory of the University of Connecticut's Marine Sciences Institute continue to pursue their study of the bubbles produced by breaking waves, and of the role these bubbles play in marine aerosol production and in the air-sea transfer of radiatively important gases.

★

Mingzhi Lu holds the B.S. (atmospheric physics) degree from Nanjing University (1983) and the M.S. degree from the Graduate School of the Chinese Academy of Sciences, Beijing, China (1986). He worked as a Research Assistant in the Institute of Atmospheric Physics of the Chinese Academy of Sciences. He is currently a graduate student in the Department of Marine Sciences, University of Connecticut at Avery Point.